

The LINC-NIRVANA Fringe and Flexure Tracker: Testing Piston Control Performance

Steffen Rost, Thomas Bertram, Bettina Lindhorst, Christian Straubmeier, Evangelia Tremou,
Yeping Wang, Gunther Witzel, Andreas Eckart

I. Physics Institute, University of Cologne, Zùlpicher Str. 77, 50937 Cologne, Germany

ABSTRACT

LINC-NIRVANA is the NIR homothetic imaging camera for the Large Binocular Telescope (LBT). Its Fringe and Flexure Tracking System (FFTS) is mandatory for an efficient interferometric operation of LINC-NIRVANA: the task of this cophasing system is to assure a time-stable interference pattern in the focal plane of the camera.

Differential piston effects will be detected and corrected in a real-time closed loop by analyzing the PSF of a guide star at a frequency of 100Hz-200Hz. A dedicated piston mirror will then be moved in a corresponding manner by a piezo actuator. The long-term flexure tip/tilt variations will be compensated by the AO deformable mirrors.

A testbed interferometer has been designed to simulate the control process of the movement of a scaled piston mirror under disturbances. Telescope vibration and atmospheric variations with arbitrary power spectra are induced into the optical path by a dedicated piezo actuator. Limiting factors of the control bandwidth are the sampling frequency and delay of the detector and the resonance frequency of the piston mirror. In our setup we can test the control performance under realistic conditions by considering the real piston mirrors dynamics with an appropriate software filter and inducing an artificial delay of the PSF detector signal. Together with the expected atmospheric OPD variations and a realistic vibration spectrum we are able to quantify the piston control performance for typical observation conditions. A robust control approach is presented as result from in-system control design as provided by the testbed interferometer with simulated dynamics.

Keywords: LBT, LINC-NIRVANA, fringe tracking, piston, control

1. INTRODUCTION

The Fringe and Flexure Tracking System^{1,2} of LINC-NIRVANA^{3,4} is a real-time servo system⁵ that allows to compensate atmospheric and instrumental optical pathlength differences (OPD). To sense these varying phase offsets (differential piston), it fits an analytic model to the profile of the point-spread function (PSF) of a suitable reference star.^{2,6} A Piston mirror is used as actuator in the fringe control loop to counteract the measured differential piston.

The sky coverage of LINC-NIRVANA is closely related to the performance of the fringe tracking system.⁶ A residual piston of 0.1λ for the central wavelength of the science band is the performance goal for the FFTS. The resulting fringe contrast should then allow for highest-resolution post-processing of the scientific images.⁷ The piston performance in turn is related to many parameters, as we show in the following.

The piston error budget due to the control loop effects is analyzed with a simulation of the expected system response. The piston signal which has to be corrected for consists of the atmospheric and the instrumental piston, including vibrations of the telescope structure and flexure effects. An overview of the FFTS system and the control tasks is given in Fig. 1. The different aspects of the piston spectrum and the appropriate control techniques are discussed in the following. With a detailed model a controlling strategy and parameters can be optimized. On the other hand the limiting reference star magnitude and distance to the target can be estimated if a residual piston performance is specified.

Send correspondence to S. Rost: E-mail: rost@ph1.uni-koeln.de, Telephone: +49 (0)221 470-3548

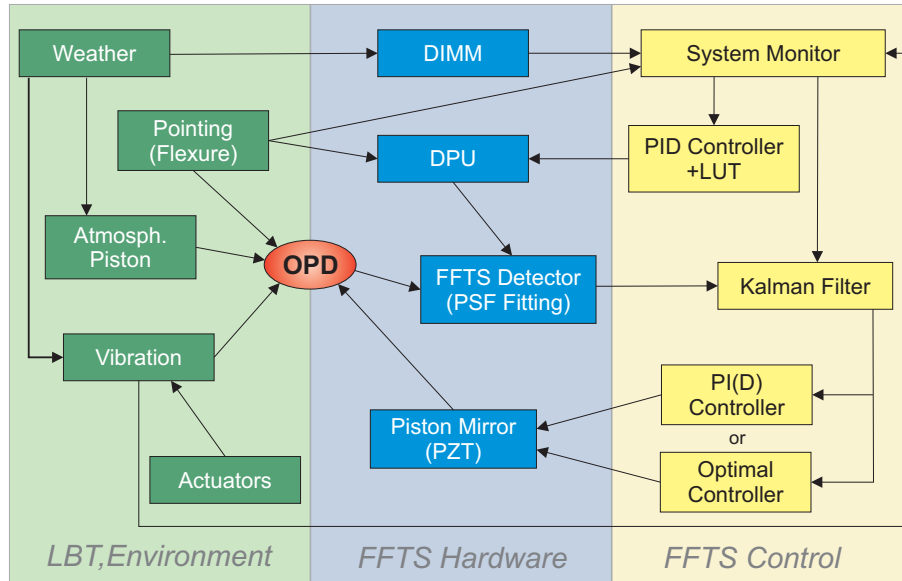


Figure 1. Overview of the FFTS control system. The task of the FFTS is to compensate atmospheric and instrumental piston or OPD. The actuators are the detector positioning unit (DPU) for the tracking of reference stars and the piston mirror. The FFTS detector for the PSF fitting and eventually a DIMM are sensors, which provide the set points for the controllers. The noisy OPD measurement is Kalman filtered for optimal piston estimation, limited dynamics of the piston mirror actuator might impose an optimal control approach.

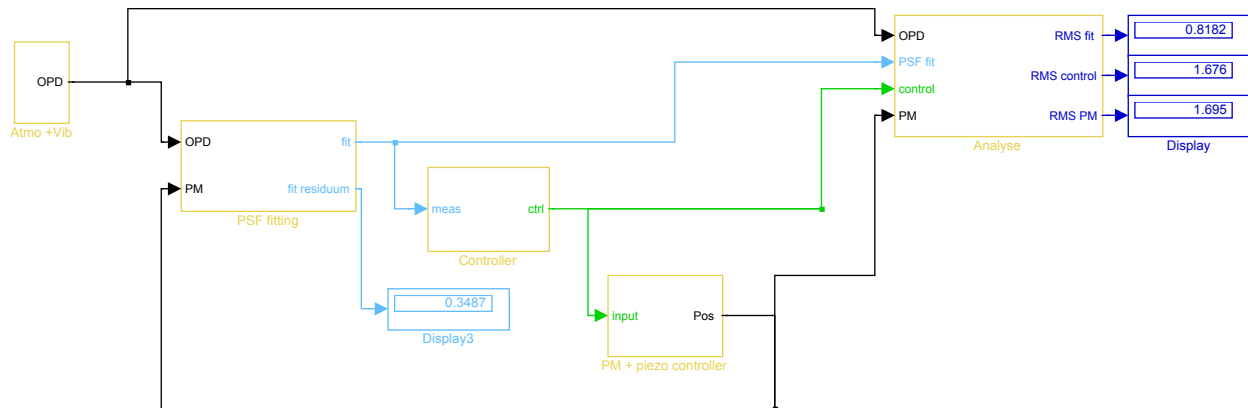


Figure 2. SIMULINK model for the simulation of the control loop performance with different atmospheric conditions and disturbances from sampling effects, latencies, PSF-fit noise and telescope vibrations. A dynamic model for the piezo actuator with piston mirror load includes the PI-control algorithm of the piezo controller.

2. SIMULATION SETUP

The residual piston and with it the performance of the LINC-NIRVANA instrument is affected by many parameters. To investigate the performance under different conditions a simulation framework was set up as a MATLAB/SIMULINK model (Fig. 2). In the following an overview of the framework is given. Figure 2 shows the SIMULINK model for the FFTS control loop.

2.1 Atmospheric piston

The OPD (optical path difference) due to the atmospheric conditions is simulated with a seven layer atmospheric model (LOST⁸) including MCAO compensation. For a detailed overview on the simulations probing standard

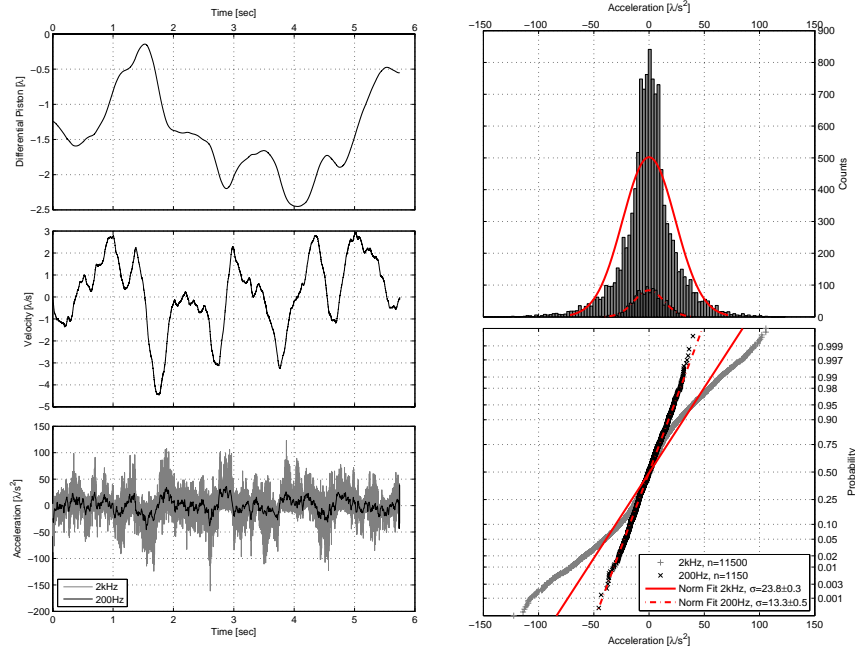


Figure 3. Left: atmospheric differential piston sequence obtained from simulations of excellent seeing conditions with the Paranal 0.3" @V-band $C_N^2(h)$ -profile. Shown are the total piston from atmosphere, the velocity and acceleration. The sampling time is $5 \cdot 10^{-4}$ s and $5 \cdot 10^{-3}$ s respectively. The acceleration is smoothed by the lower sampling rate. Right: The probability distribution of the variation in acceleration. To the top the histogram and fitted normal density function, to the bottom the cumulative distribution function and normal fits. The distribution differs from the normal distribution, but the deviations are small in the case of low sampling rates.

and extreme cases see Bertram et al.⁶ In the following atmospheric conditions with a seeing of 1.5", 0.7" (San Pedro Martir $C_N^2(h)$ -profile) and 0.3" (Paranal profile) are assumed. The OPD time series over 6 seconds is then resampled with the corresponding framerate of the FFTS-detector and a delay is added, due to the detector read-out, A/D-conversion, OPD algorithm CPU-time, etc.⁵ Because of the time-consuming simulation of the atmosphere a direct interface from LOST (IDL) to MATLAB was skipped. Pre-computed simulations of representative seeing conditions are used as atmospheric piston input.

In figures 3– 5 a statistical analysis of the second derivative of the piston is shown, i.e. the piston "acceleration". The actual variation of this value is important for the control parameters.

2.2 Instrumental piston

For the instrumental piston from vibration (and eventually flexure) the simulated piston signal is mixed with oscillations of arbitrary frequencies and amplitudes. Extensive measurements of vibrations at the LBT indicate power spectra with certain critical frequencies, i.e. around 3 Hz, 12Hz, and 15Hz. The measurements and preliminary results are presented in Brix et al.⁹ The actuator of the piston mirror should allow movements with the measured frequencies and amplitudes of the vibrations in terms of dynamics and travel range. Nevertheless the simulations indicate, that with increasing complexity of the vibration spectrum –i.e. many uncorrelated frequencies– the vibration control becomes difficult.

2.3 Piston measurement disturbance

2.3.1 PSF fitting

Bertram et al.⁶ developed an image analysis concept with a multidimensional PSF-fitting algorithm. Differential piston can be determined even with a low signal-to-noise ratio (SNR). Nevertheless the quality of fit will decrease with decreasing SNR, which in turn is dominated by the detector readout noise. Thus the frame rate of the detector is a tradeoff between sampling rate and measurement error of the piston signal. As the sampled signal

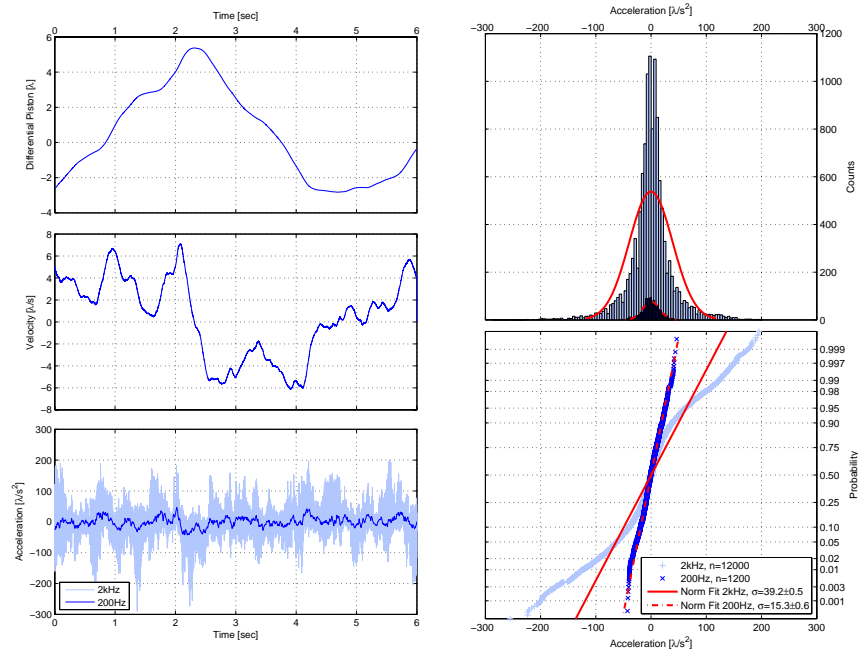


Figure 4. Same as figure 3, but for average seeing (San Pedro Martir 0.7''@V).

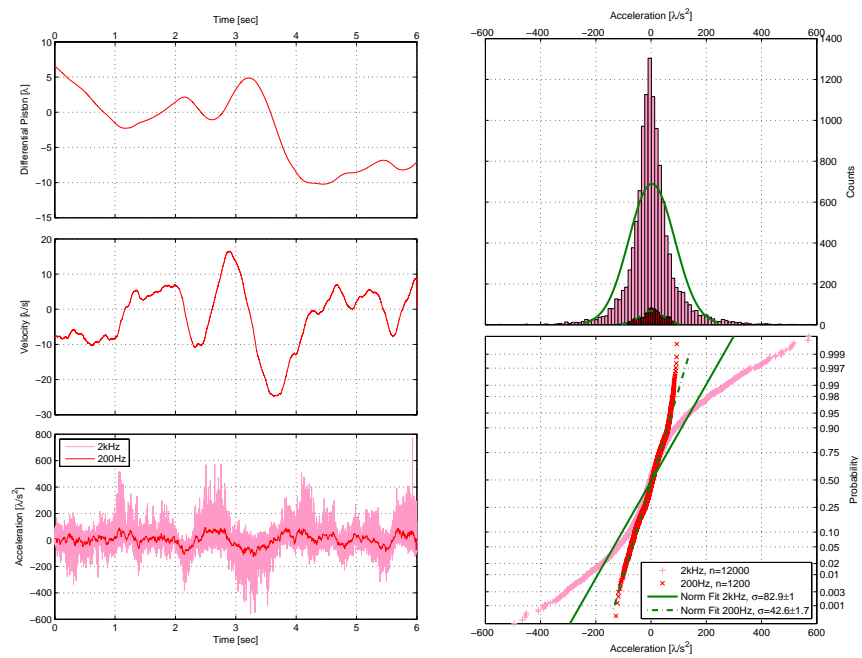


Figure 5. Same as figure 3, but for bad seeing (San Pedro Martir 1.5''@V).

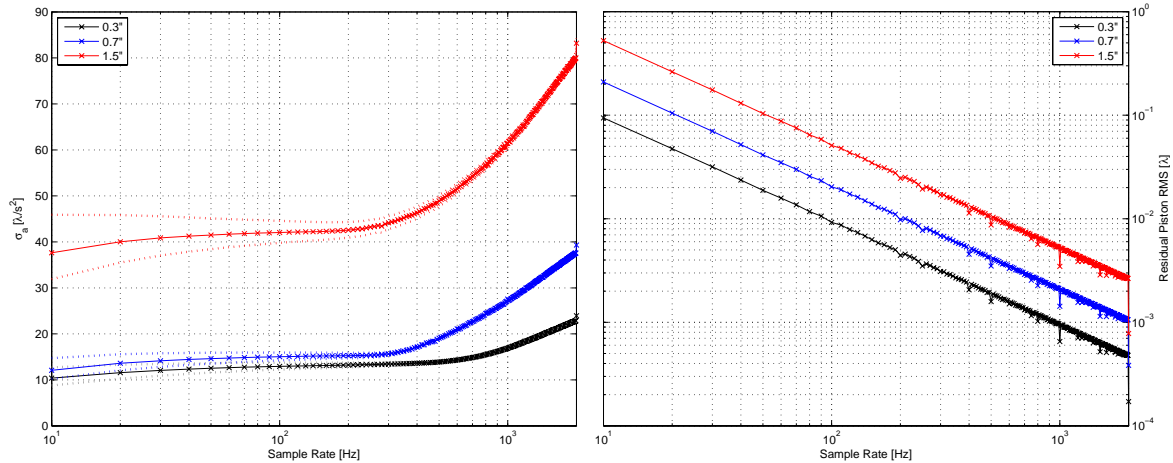


Figure 6. Left: Piston variation as a function of sample rate. The variation is the standard deviation of the fitted normal distribution of the down-sampled piston acceleration. Base sample rate of the piston sequence is 2kHz. In the region of achievable piston sampling of 50–200Hz a nearly constant value can be assumed. The reconstructed piston signal is less varying with lower sample rate as the real piston sequence is smoothed by the down-sampling. The residual error is shown in the plot to the right, for instance for average seeing (0.7 λ) at 200Hz the piston performance will not exceed $\sim 0.01\lambda$.

is also delayed, extrapolation or prediction performance is important. With increasing noise due to the fitting, the prediction becomes difficult. The disturbances of the piston measurement are simulated in the corresponding block of the SIMULINK model.

The OPD is measured with the FFTS-detector at a fixed frame rate which is limited by the magnitude of the reference star. The higher the magnitude the greater the DIT to achieve a reasonable SNR. The SNR of the reference star PSF has a strong impact on the piston analysis performance and requires therefore a minimum exposure time. The achieved frame rate with an image size of 32×32 pixels is 100-200 Hz. The piston power spectrum which can be corrected for is therefore limited to the Nyquist frequency (50-100 Hz). With no knowledge of the behavior of the piston in between the samples, the FFTS performance will decrease with lower sampling rates (Fig. 6).

2.3.2 Sampling rate

To classify the discrete sampling of a signal as disturbance is somewhat misleading. Nowadays nearly all information and measurement is acquired, processed and stored in digital form and therefore sampled in some way. According to the Nyquist-Shannon theorem for complete reconstruction the lowest sampling frequency of a continuous signal is greater than twice the bandwidth.

It is evident, that for every process with virtually unlimited bandwidth information is lost by discrete sampling. The signal has to be low-pass filtered with the Nyquist-frequency to avoid aliasing effects.

Down-sampling the piston signal at a rate of 100–200Hz is equivalent to a smoothing, so the variation is decreased. The down-sampled signal resembles an even closer to normal distribution in piston variation, naturally with a decreased standard deviation (cf. Figs. 3– 5). In figure 6 to the left the change in variation or the degree of smoothing is shown. In the achievable range of the sampling rate for the FFTS the variation can assumed to be constant. The residual error which cannot be corrected for increases with lower sampling rates, as the control bandwidth is decreased. This is shown in figure 6 to the right. This residual error – assuming that the piston variation obtained from the simulations at 2kHz is realistic and quasi-continuous – is an upper limit for the performance, which can be achieved with the FFTS.

2.3.3 Latencies

Because of the integration time of the PSF image acquisition, the read-out time, A/D-conversion and image analysis the piston signal is also delayed. The estimated latencies during the analysis of the piston sum up to

a delay of $\tau_s \sim 8\text{ms}$.⁵ For stable control the latency should be kept as small as possible, but also a constant delay is desired, i.e. no jitter of the processing time. Wang et al.¹⁰ examined the latency variance on a real-time computer system and introduced a software solution for fast and time stable data processing.

3. CONTROL LAW

3.1 Requirements

The final control algorithm for the FFTS has to fulfill some requirements arising from the complex and varying disturbance conditions. It should have a temporal prediction ability to compensate for the inevitable delay due to the detector integration/readout time and the image processing. The prediction ideally bridges the gap between samples of the piston signal with a time-dependent extrapolation, so that the control signal is a smooth curve based on the most likely piston state and variation. As a consequence the control loop will operate with a much higher sampling rate than the image acquisition, probably limited by the available real-time processing power. Model uncertainties such as the underlying piston power spectrum, measurement covariances and the system dynamics must not affect the overall performance too much or even lead to control un-stabilities such as steady state errors. These offset errors, as well as phase shifts, substantial overshooting and temporal un-stabilities can severely reduce the fringe contrast over the science detector integration time (DIT). Residual piston from conservative and less aggressive control setups will also decrease the performance. The primary objective of the control design is to achieve precise tracking of almost arbitrary input signals with high control bandwidth in spite of external disturbance.

The variations in input conditions are not known or predictable, so the algorithm itself should not be very complex or abstract, as only simplified simulations can be tested during the design. With exotic control approaches, e.g. neural networks untested input states and sequences can eventually cause a inconsistent state of the controller which can result in total performance breakdown.

3.2 Optimal control

The term optimized controller refers to a mathematical optimization, i.e. minimization of a cost function, which is defined in a way to evaluate the performance of a control system. A controller is therefore optimized only in terms of a given performance weighting.

Considering the limited bandwidth of the actuator due to the piston mirror load a more sophisticated control approach than the standard PID controller might significantly improve the performance. A tuned controller for the specific problem should be an advantage, but also implies a specific, probably complex hardware design.

The parametric model of the piston mirror and actuator is based on frequency response measurements.⁵ The weights are defined as:¹¹

- W_3 weights the sensitivity function $S = 1/(1 + GK)$, and when W_3S is minimized in the \mathcal{H}_∞ norm, the residual control error is limited.
- W_2 weights the complementary sensitivity function $T = I - S$, minimizing W_2T avoids sensitivity to noise and results in robustness.
- W_1 weights the controller output $u = KSw$, so minimizing W_3KS penalizes large plant inputs w and effectively limits the controller output, i.e. a gain margin.

The optimization problem can then be written as

$$\gamma = \min_K \|N(K)\|_\infty, \quad N = \begin{pmatrix} W_1KS \\ W_2T \\ W_3S \end{pmatrix}, \quad (1)$$

i.e. to find the controller K which minimizes the \mathcal{H}_∞ norm. To the left of figure 7 the weighting functions W_2^{-1} and W_3^{-1} are shown for a desired bandwidth of 150Hz, weighting with W_1 was omitted.

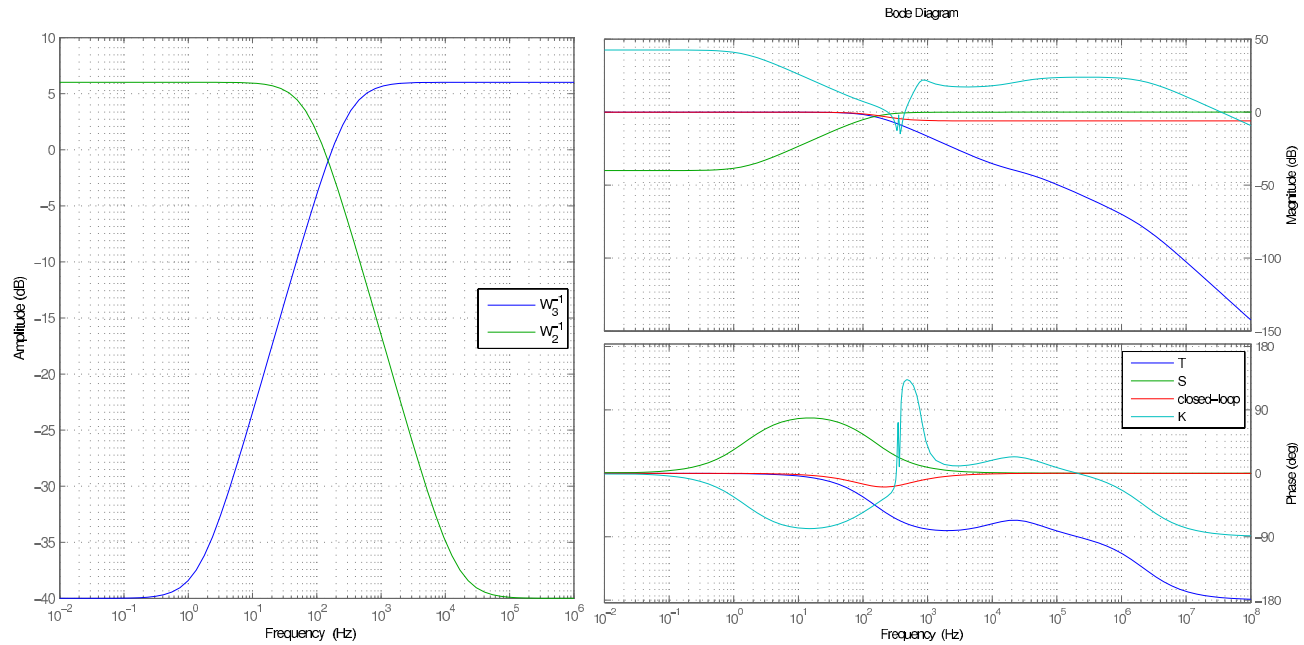


Figure 7. The inverse weighting functions for application of the \mathcal{H}_∞ norm are shown to the left for a desired bandwidth of 150Hz. Right: result of the optimization. The shaped controller K (turquoise line) is similar to the inversion of the system G . The achieved closed-loop transfer function (red line) is nearly flat.

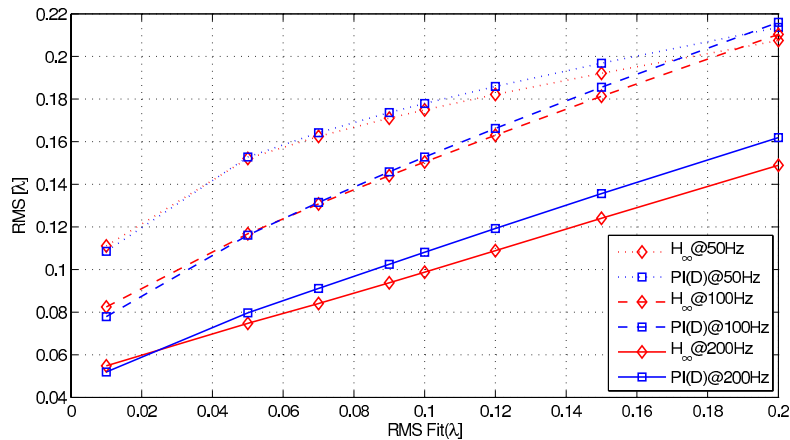


Figure 8. Performance simulation of the \mathcal{H}_∞ controller in comparison to a tuned PI(D). Shown is the residual OPD error (RMS) as a function of PSF fitting error for sampling rates 50, 100 and 200 Hz.

The evaluation of Eqn. 1 and the shaping of the controller K is done in MATLAB with the two-Riccati formulae¹² and a γ -iteration technique to find the optimal value of γ , i.e. the defined cost. The obtained controller and the closed-loop transfer function are shown in Fig. 7. In direct comparison with the tuned PI(D) the optimized controller is shown in figure 8. Indeed a performance advantage is seen. Especially under difficult conditions with increased measurement noise \mathcal{H}_∞ provides a decreased residual piston. It is clear, that the greatest improvement is achieved at 200Hz, since this sampling rate imposes control signals with higher frequencies than the resonance frequency. As a conclusion, it might be worth to design a new hardware controller which incorporates the simulation results.

3.3 Piston estimation

There are many possibilities to reconstruct a sampled signal. The most simple is the zero-order-hold (ZOH) technique, which implies holding the last value constant until the next measurement. The control signal and the

residual piston can be improved with a simple predictor. After the PSF fitting algorithm the signal is resampled to a higher sampling rate (e. g. 2 kHz). By evaluating the derivative for the last n samples the trend of the piston can be extrapolated. The extrapolation also takes care of the latency by evaluating the time $t + \tau_s$. The resulting discontinuities can be compensated with a discrete (low-pass) filter. This approach can improve the control performance significantly for the case of an undisturbed signal.⁵

However, the piston prediction based on extrapolation is inappropriate for a disturbed signal, i.e. the noisy measurement of the piston with PSF fitting. The consideration of the error of the piston measurement as well as the underlying physical model leads to the formal description of the optimal estimator, the Kalman filter. An improvement of the simple prediction filter algorithm can be achieved, if a priori knowledge of the system is considered. Nowadays Kalman filtering is often applied to challenging control tasks and also used in telescope engineering.^{13,14}

The Kalman filter is formulated in the discretised time domain. The assumption for the linear dynamical system is, that given a state x_k in the present, the future state x_{k+1} is completely independent of the past state x_{k-1} .

In the current implementation of the filter to estimate the atmospheric piston the system is assumed to obey linear dynamics. That means that the piston state x can be described by the instantaneous piston ϵ and the first derivative, i.e. the velocity

$$x = \begin{pmatrix} \epsilon \\ \dot{\epsilon} \end{pmatrix}. \quad (2)$$

The state transition matrix for the time step Δt is constant

$$F(\Delta t) = \begin{pmatrix} 1 & \Delta t \\ 0 & 1 \end{pmatrix}. \quad (3)$$

Since the filter is formulated in the discrete time domain, the variation analysis of simulated piston sequences in figures 3– 5 was done in the time domain rather than in the frequency domain. It is also important, that the variation differs not too much from the normal distribution, since the Kalman filter assumes white process noise. The covariance of the process noise can therefore be denoted with the piston acceleration σ_a , as investigated for representative atmospheric conditions. The process noise is then denoted with

$$Q = \sigma_a^2 G G^T, \quad G = \begin{pmatrix} \frac{\Delta t^2}{2} \\ \Delta t \end{pmatrix}. \quad (4)$$

The covariance of the observation noise is $R_k = \sigma_{\text{fit}}^2$, the piston fit error, dependent on the reference star magnitude and DIT. Figure 9 shows the dependence of the performance on σ_a and on the PSF fitting error σ_{fit} .

Since the Kalman filter is capable of processing any available measurements regardless of their precision, it would also be possible to incorporate piston estimates from the MCAO system. A software interface to the corresponding control system, which provides the AO correction information might improve estimates of the piston state and the variation. The current implementation of the filter allows an easy extension of the measurement inputs.

The prediction of the piston inbetween samples takes advantage of the estimated state, including the velocity $\dot{\epsilon}$. After the updating phase k of the filter the actual piston is then evaluated due to the latency τ_s in the time range $t_k \leq t \leq t_{k+1}$ until the next prediction/updating phase with

$$x(t) = F(t + \tau_s)x_k. \quad (5)$$

3.4 Adaptive Control

The standard deviation of the piston as well as the temporal variation scale with the seeing conditions. A differential image motion monitor (DIMM) is planned to be installed at the LBT dome to steadily monitor the atmospheric seeing during an observation. Additional improvement of the performance of the piston estimation

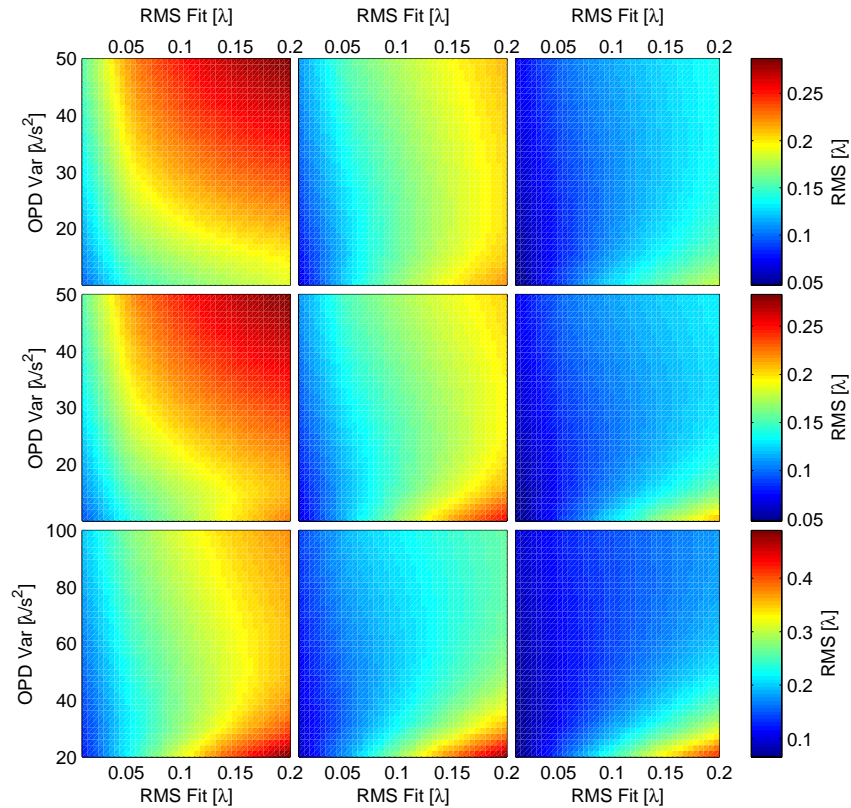


Figure 9. Performance simulation of the Kalman filter. Shown is the residual OPD error (RMS) as a function of PSF fitting error and OPD variance as the parameter for the Kalman filter. From left to right for sampling rates 50, 100 and 200 Hz. From top to bottom for 0.3", 0.7" and 1.5" seeing conditions. The latency is 8 ms.

could be achieved, if the actual measured seeing is fed into the control loop, precisely into the Kalman filter. The filter weights its prediction with the covariance of the process noise. If the DIMM communicates an expected low variation (due to a moderate seeing), the filter will be adapted to predominantly reject higher variations, because these are assumed to be mainly contributions from measurement noise. A corresponding interface is foreseen in the current implementation of the filter algorithm, so once the DIMM is installed and working – as well as the FFTS and LINC-NIRVANA – this can be tested under realistic conditions. The look-up tables to evaluate the optimal covariances as a function of r_0 are obtained from the LOST simulations of the representative C_n^2 profiles of seeings 0.3", 0.7" and 1.5" (cf. Fig. 9).

The same principle can be applied to the vibration compensation. The current measurement setup,⁹ in principle, allows to steadily monitor phases and amplitudes of vibrations. If it is feasible to feed the measurements in real-time into the control-loop, the vibrations could be compensated effectively.

4. TESTBED INTERFEROMETRY

A testbed interferometer, set up as laboratory experiment, is used to develop the FFTS control loop and to test the robustness of the fringe tracking concept. The geometry of the resulting interferometric intensity distribution in the focal plane of the implemented CCD corresponds to that of the LBT PSF. The setup allows to produce monochromatic (He-Ne laser) and polychromatic (halogen lamp) PSFs and allows to actively introduce well defined low-order phase perturbations, namely OPD and differential tip/tilt. Furthermore, all components that are required in a fringe tracking servo loop are included: a sensor for fringe acquisition and an actuator to counteract measured OPD. With this setup it is intended to determine the performance with which a fringe tracking control loop is able to compensate defined OPD sequences, to test different control algorithms, and to

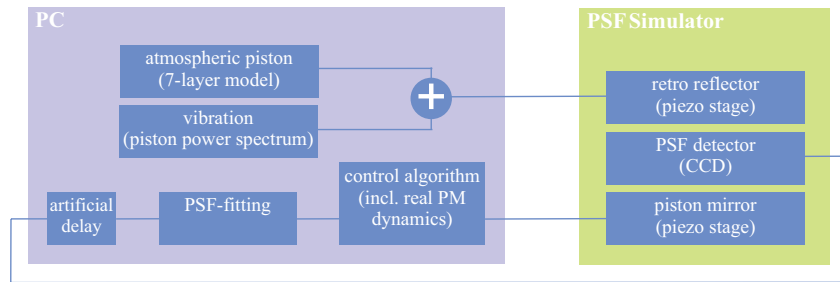


Figure 10. Scheme of the PSF simulator system to simulate the FFTS performance. The disturbances of the control signal are considered with the simulated atmospheric piston and the telescope vibration power spectrum. Additionally a realistic delay and PSF fitting noise is achieved in software. The hardware actuator and sensor are used in real-time to test the overall long-term stability of the system.

optimize the control parameters of an existing servo system. The system is described in detail in Bertram et al.¹⁵

The purpose of the testbed is to integrate the hardware and software in a system, which allows tests of the robustness of the fringe tracking concept. The current setup replicates nearly the complete hardware of the FFTS, as only the detector positioning unit (DPU) is missing, and performance effects due to flexure and tracking errors of this device can not be considered (cf. Fig. 1). The used CCD detector is slower ($\sim 30\text{Hz}$) as the FFTS detector and has a different latency, but scaling of the system dynamics is possible. Piston sequences or a signal piston generated from a specified temporal piston variation and vibrations according to the assumed vibration power spectrum can be introduced at the retro-reflector actuator. The two processes of introducing controlled OPD and the compensation in the PSF fitting loop are independent. Realistic detector conditions can be achieved by applying noise levels, exposure time variation, etc., to test the PSF fitting algorithm for arbitrary observation conditions (Fig. 10). The software of the system is the same as for the final FFTS, except the different hardware interfaces.

After precise alignment of the setup fringes are detected as expected. First coherence length and scanning tests for the zeroth fringe determination revealed multiple reflections, which are not clearly identified yet.¹⁵ The software development is in progress, but first piston tracking experiments are promising and confirm the consideration of sophisticated control techniques, i.e. optimal estimation of the noisy measurement, delay compensation by prediction and the optimal feedback control for the limited non-linear dynamics, which provides stability and disturbance rejection.

The testbed interferometer allows for the design and optimization of control approaches and stability tests of the software under realistic conditions, at the same time as the hardware construction and testing phase of the FFTS is initiated. This procedure will speed-up the integration process into LINC-NIRVANA and the final installation at the LBT.

5. DISCUSSION

The presented simulation framework allows the investigation of residual piston and with it the overall performance of the LINC-NIRVANA instrument due to control effects and system response. It is an important supplement to the considerations of the piston error budget due to the optical system.^{7, 16, 17}

Together with the atmospheric simulations of LOST, a nearly complete system model is provided, from the arising of piston between the two apertures to the actual achievable piston compensation with the piston mirror. It emerged that many correlated parameters affect the performance, the best parameter setup depends on the actual observing conditions. Simulations of assumed conditions could help to set optimized parameters: which reference star should be picked? Which band is best-suited for tracking? Which is the optimal sampling rate as a trade-off between better SNR or more samples and better reconstruction? The generation of parameter tables is an ongoing process of estimation of optimal setups for specific observation conditions. More detailed look-up tables provide a better understanding of system responses.

A satisfactory solution of OPD compensation due to vibration is not achieved yet. More measurements have to be done, as the telescope's completion is advancing. The approach to realize real-time monitoring with phase information, might provide – if feasible – the easiest way of compensation. Definitely it will help to design more efficient vibration filters and (Kalman) estimators.

Optimal control is advisable for the non-linear PZT actuator, the intrinsic disturbance rejection is crucial for the system to avoid ruined science exposures, since telescope time is expensive. The hardware design might impose additional difficulties and effort, though. Further improvement of the controller design could involve advanced modeling with uncertainties, which provides additional robustness. \mathcal{H}_∞ already avoids problems due to uncertainties at high frequencies by the proper weighting functions. Hence the modeling is not too critical at that regime, the need for precise measurements and modeling is relaxed.

The further development of the FFTS includes tests of software and control robustness in a realistic physical system. Several techniques, such as the image analysis including the PSF fitting, the software real-time concepts and the control approach have to be reconfirmed as part of the whole, complex system, before the integration of the FFTS into the LINC-NIRVANA instrument takes place. The testbed interferometer is a valuable tool for this first integration phase.

ACKNOWLEDGMENTS

This work is supported in parts by the Deutsche Forschungsgemeinschaft (DFG) via grants SFB 494, HBFG #111-519 & #111-520, and Verbundforschung 05AL2PLA/5 & 05AL5PKA/0.

REFERENCES

- [1] Bertram, T., PhD thesis, Universität zu Köln (October 2007).
- [2] Bertram, T., Eckart, A., Lindhorst, B., Rost, S., Straubmeier, C., Wang, Y., Wank, I., Witzel, G., Beckmann, U., Brix, M., Egner, S., and Herbst, T. M., “The LINC-NIRVANA fringe and flexure tracking system,” *Proc. SPIE* **7013-78** (2008).
- [3] Herbst, T. M., Ragazzoni, R., Eckart, A., and Weigelt, G., “The LINC-NIRVANA interferometric imager for the Large Binocular Telescope,” *Proc. SPIE* **5492**, 1045–1052 (Sept. 2004).
- [4] Herbst, T. M., Ragazzoni, R., Eckart, A., and Weigelt, G. P., “LINC-NIRVANA: the Fizeau interferometer for the LBT,” *Proc. SPIE* **7013-77** (2008).
- [5] Rost, S., Bertram, T., Straubmeier, C., Wang, Y., and Eckart, A., “The LINC-NIRVANA fringe and flexure tracker: piston control strategies,” *Proc. SPIE* **6274-1P** (2006).
- [6] Bertram, T., Arcidiacono, C., Straubmeier, C., Rost, S., Wang, Y., and Eckart, A., “The LINC-NIRVANA fringe and flexure tracker: image analysis concept and fringe tracking performance estimate,” in [*Advances in Stellar Interferometry. Edited by Monnier, John D.; Schöller, Markus; Danchi, William C.. Proceedings of the SPIE, Volume 6268, pp. 62683P (2006).*], Presented at the Society of Photo-Optical Instrumentation Engineers (SPIE) Conference **6268** (July 2006).
- [7] Desidera, G., La Camera, A., Boccacci, P., and Carillet, M., “General performance analysis of a Fizeau interferometer,” *Proc. SPIE* **7013-147** (2008).
- [8] Arcidiacono, C., Diolaiti, E., Ragazzoni, R., Farinato, J., and Vernet-Viard, E., “Sky coverage for layer-oriented mcao: a detailed analytical and numerical study,” *Advancements in Adaptive Optics* **5490**(1), 563–573, SPIE (2004).
- [9] Brix, M., Naranjo, V., Beckmann, U., Bertram, R., Bertram, T., Brynnel, J., Egner, S., Gaessler, W., Herbst, T. M., Kuerster, M., Rohloff, R. R., Rost, S., and Schmidt, J., “Vibration measurements at the Large Binocular Telescope (LBT),” *Proc. SPIE* **7012-92** (2008).
- [10] Wang, Y., Bertram, T., Straubmeier, C., Rost, S., and Eckart, A., “The LINC-NIRVANA fringe and flexure tracker: Linux real-time solutions,” in [*Advanced Software and Control for Astronomy. Edited by Lewis, Hilton; Bridger, Alan. Proceedings of the SPIE, Volume 6274, pp. 62741O (2006).*], Presented at the Society of Photo-Optical Instrumentation Engineers (SPIE) Conference **6274** (July 2006).
- [11] Skogestad, S. and Postlethwaite, I., [*Multivariable Feedback Control*], John Wiley & Sons (2005).

- [12] Doyle, J. C., Glover, K., Khargonekar, P., and Francis, B., "State-space solutions to standard H_2 and H_∞ control problems," *IEEE Transactions on Automatic Control* **34**, 831–847 (Aug. 1989).
- [13] Le Roux, B., Ragazzoni, R., Arcidiacono, C., Conan, J.-M., Kulcsar, C., and Raynaud, H.-F., "Kalman-filter-based optimal control law for star-oriented and layer-oriented multiconjugate adaptive optics," in [*Advancements in Adaptive Optics. Edited by Domenico B. Calia, Brent L. Ellerbroek, and Roberto Ragazzoni. Proceedings of the SPIE, Volume 5490, pp. 1336-1346 (2004).*], Bonaccini Calia, D., Ellerbroek, B. L., and Ragazzoni, R., eds., *Presented at the Society of Photo-Optical Instrumentation Engineers (SPIE) Conference* **5490**, 1336–1346 (Oct. 2004).
- [14] Petit, C., Quiros-Pacheco, F., Conan, J.-M., Kulcsar, C., Raynaud, H.-F., Fusco, T., and Rousset, G., "Kalman-filter-based control for adaptive optics," in [*Advancements in Adaptive Optics. Edited by Domenico B. Calia, Brent L. Ellerbroek, and Roberto Ragazzoni. Proceedings of the SPIE, Volume 5490, pp. 1414-1425 (2004).*], Bonaccini Calia, D., Ellerbroek, B. L., and Ragazzoni, R., eds., *Presented at the Society of Photo-Optical Instrumentation Engineers (SPIE) Conference* **5490**, 1414–1425 (Oct. 2004).
- [15] Bertram, T., Lindhorst, B., Tremou, E., Rost, S., Wang, Y., Witzel, G., Straubmeier, C., and Eckart, A., "The LINC-NIRVANA Fringe and Flexure Tracker: The testbed interferometer," *Proc. SPIE* **7013-117** (2008).
- [16] Egner, S., Herbst, T. M., and Arcidiacono, C., "General performance analysis of a Fizeau interferometer," *Proc. SPIE* **7013-122** (2008).
- [17] Pavlov, A. I. and Gaessler, W., "The performance estimator in the framework of the LINC-NIRVANA observation preparation software," *Proc. SPIE* **7013-116** (2008).